Iraqi National Journal of Earth Science
www.earth.mosuljournals.com

Borehole Seismic Test and Seismic Surface Waves Survey for Site-Specific Investigation at Al Layyah Power Generation Plant, Sharjah, United Arab Emirates

Ahmed J. R. Al-Heety [1*], Zainab M. Shanshal [2], Mohammed Hassouneh [3] Kamal Abdelrahman[4], Sherif M. Ali [5], Biman K. Dey [6]

[1] *Seismic Processing Center/ Oil Exploration Company, Baghdad, Iraq.*
[2] *Department of Geology, College of Sciences, University of Mosul, Mosul, Iraq.*
[3,6] *Tatweer for Geophysical Studies and Consulting (TGSC), Abu Dhabi, U.A.E.*
[4] *Department of Geology & Geophysics, College of Science, University of King Saud, Saudi Arabia.*
[5] *National Research Institute of Astronomy and Geophysics (NRIAG), 11421 Helwan, Cairo, Egypt.*

Article information

Received: 22- Jan -2024

Revised: 04- Mar -2024

Accepted: 24- Mar -2024

Available online: 01- Jan – 2025

Keywords:
Shear-wave velocity
Surface wave
MASW
Borehole measurements

Correspondence:
Name: Ahmed J. R. Al-Heety

Email: ahmedalheety@gmail.com

ABSTRACT

Integrated geophysical seismic measurements have been carried out at Al Layyah Power Generation Plant site, Sharjah, United Arab Emirates to determine the geotechnical properties of soil/rocks. The CHST is performed within a group of 3 boreholes, while a DHST is conducted at one site to determine a velocity profile. Active Multichannel Analysis of Surface Waves (MASW) data is carried out along one MASW line with a total length of 40 m. The measurements have been carried out between boreholes BH-03 and BH-04 along the asphaltic road at the study site. The estimating of dynamic soil properties from the outcomes of seismic surveys is discussed utilizing the seismic velocity acquired from the three locations. The processing and analysis of data and correlation with geological information are described based on the comparative evaluates of the corresponding 1D Vs profiles; it is concluded that CHST and DHST data are generally more reliable than MASW data. 1D Vs profiles obtained from MASW, CHST, and DHST are compared and the average Vs of the top 30 m (Vs30) is computed. There are similar up to 30 m of Vs profiles gained in all seismic tests. Consequently, a good quality recording, processing, and interpretation of MASW data allows dependable results and the same classification of the soil. It indicates that the Vp and Vs have a good correlation with the borehole log. Moreover, the site soil classification is found to be C (Very dense soil and soft rock profile) according to the Dubai Municipality Building Code (DIBC-2004) and the International Building Code (IBC 2009).

DOI: 10.33899/earth.2024.146196.1222,

تطبيق طريقة قياس سرع الموجات الزلزالية عبر الابار وتحليل مسح الموجات السطحية الزلزالية للتحريات الموقعية في محطة الليّة لتوليد الطاقة، الشارقة، الإمارات العربية المتحدة

أحمد جدوع الهيتي[1*]، زينب مصدق شنشل[2]، محمد حسونة[3]، كمال عبد الرحمن[4]، شريف محمد علي[5]، بيمان ك. دي[6]

[1] مركز معالجة البيانات الزلزالية، شركة الاستكشافات النفطية، وزارة النفط، بغداد، العراق.

[2] قسم الجيولوجيا، كلية العلوم، جامعة الموصل، الموصل، العراق.

[6،3] تطوير للدراسات والاستشارات الجيوفيزيائية(TGSC) ، أبو ظبي، الإمارات العربية المتحدة.

[4] قسم الجيولوجيا والجيوفيزياء، كلية العلوم، جامعة الملك سعود، الرياض، المملكة العربية السعودية.

[5] المعهد القومي للبحوث الفلكية والجيوفيزيائية (NRIAG)، حلوان، القاهرة، مصر.

معلومات الارشفة

تاريخ الاستلام: 22- يناير -2024

تاريخ المراجعة: 04- مارس -2024

تاريخ القبول: 24- مارس -2024

تاريخ النشر الالكتروني: 01- يناير -2025

الكلمات المفتاحية:

سرعة موجة القص

موجة سطحية

التحليل متعدد القنوات للموجات السطحية

قياسات عبر الآبار

المراسلة:

الاسم: أحمد جدوع الهيتي

Email: ahmedalheety@gmail.com

الملخص

تم إجراء تكامل القياسات الزلزالية في موقع محطة الليّة لتوليد الطاقة في مدينة الشارقة، دولة الإمارات العربية المتحدة لتقييم الخصائص الجيوتقنية للتربة والصخور. يتم استخدام طريقة قياس سرع الموجات الزلزالية عبر الآبار بشكل متزايد في التحريات الجيوتقنية لتقدير الخصائص الديناميكية للتربة/الصخور. تم إجراء الاختبار الزلزالي عبر الآبار ضمن مجموعة مكونة من 3 آبار لكل موقع، في حين تم إجراء اختبار مسح أسفل البئر في موقع واحد لتحديد مقطع السرعة. تم إجراء التحليل متعدد القنوات للموجات السطحية على طول خط زلزالي واحد بطول قدره 40 متراً ما بين الآبار BH-03 وBH-04 على طول الطريق الأسفلتي في موقع الدراسة. تمت مناقشة تقدير خصائص التربة الديناميكية من نتائج المسوحات الزلزالية باستخدام السرعة الزلزالية المكتسبة من المواقع الثلاثة (9 آبار). كما تم توضيح معالجة وتفسير البيانات الجيوفيزيائية والجيوتقنية وارتباطها بالوحدات الجيولوجية. واستنادًا إلى التقييمات المقارنة لمقاطع السرعة القصية، تم استنتاج أن بيانات CHST وDHST أكثر موثوقية بشكل عام من بيانات MASW. كما وتم حساب متوسط سرعة موجة القص لـ 30 مترًا (Vs30) لكل اختبار. وجد ان هنالك تقارباً بمقاطع Vs التي تم الحصول عليها من الاختبارات الزلزالية. ولذلك، فإن طريقة المسح عبر الابار وبيانات MASW تسمح بنتائج موثوقة وبنفس التصنيف الزلزالي للتربة. علاوة على ذلك، فقد وجد أن تصنيف تربة الموقع هو C (تربة ذات كثافة عالية) وفقاً لكود البناء لبلدية دبي (DIBC-2004) وكود البناء الدولي (IBC 2009).

DOI: 10.33899/earth.2024.146196.1222,

Introduction

Major cities in the U.A.E., such as Sharjah, face various fears affecting many types of infrastructure engineering projects, e.g., bridges, roads, ports, landfills, hospitals, buildings, power plants, and desalination plants. Sharjah City is the Emirate's capital and the third-most populous city in the U.A.E. after Dubai and Abu Dhabi, putting it at risk of soil subsidence that generally takes place in the coastal area, at which places of weak and soft soils are common. Soil problem situations are important for infrastructure, e.g., schools, hospitals, desalination plants, and power plants. Al Layyah Suburb, located at the southwestern edge of the Sharjah Emirate, is the home to several government offices and the famous Port Khalid.

Geotechnical works play an important role in a wide range of civil engineering projects that are concerned with construction on the surface or within the ground. The dissimilarity in

soil properties is a vital challenge in geotechnical engineering (Honjo, 2011). The source of spatial inconsistency is commonly associated with geological developments taking place in the deposition of rock and soil horizons (Phoon and Kulhawy, 1999). Generally, there are common procedures for soil and rock investigation including geophysical tests (Kearey *et al.,* 2002; Look, 2014). The geophysical operations can be executed on the ground surface or inside holes (Foti, 2012; Taylor, 1999). These geotechnical methods are intrusive, such as borehole seismic testing, and non-intrusive such as (seismic refraction, MASW).

In contrast with the borehole seismic tests (BHST), the MASW method needs not large equipment or energy sources, which is much quicker than the borehole seismic tests. On the other hand, BHST delivers further precise data about a specific area. Therefore, the ideal result is to combine the pros of these methods. BHST can deliver precise limited info. In contrast, the MASW method offers a smooth local average and must be correlated with the borehole data (Xie *et al.,* 2022).

The geophysical data grant a physical properties distribution of the sub-surface to be evaluated and compared with other properties (such as seismic velocity, density, and elastic moduli) (Foti, 2012). The Vs of soil have been correlated to many geotechnical specifications via empirical equations and relations (e.g., Wair *et al.,* 2012; Kramer, 2014; Hussien and Karray, 2015; Moon and Ku, 2016; L'Heureux and Long, 2017). The seismic velocities together with the density are used to evaluating the in-situ elastic and dynamic parameters of soils.

There are several geophysical approaches for the evaluation of in-situ Vp and Vs and obtaining a 1D vs. depth profile or 2D vs. cross-sections versus depth. Among the geophysical techniques employed to investigate soil or rock are seismic refraction (for Vp) and shear refraction (for Vs), surface wave analysis (Vs), crosshole (CHST), and downhole (DHST) seismic tests (for Vp and Vs) (e.g., Foti *et al.,* 2014; Al-Saigh and Al-Heety, 2013; Al-Heety, 2016; Garofalo *et al.,* 2016a; 2016b).

The BHST and MASW methods are applied rather than conventional seismic methods and successfully influenced to geotechnical topics that the shear wave velocity structure to be produced (Al-Heety *et al.,* 2021). This essential property can be gained using BHST (Sairam *et al.,* 2019), and MASW methods (Socco and Strobbia, 2004; Martínez-Pagán *et al.,* 2018; Abdelrahman *et al.,* 2020). Figures (1 and 2) show schematics of the CHST, DHST, and typical MASW measurement layouts respectively.

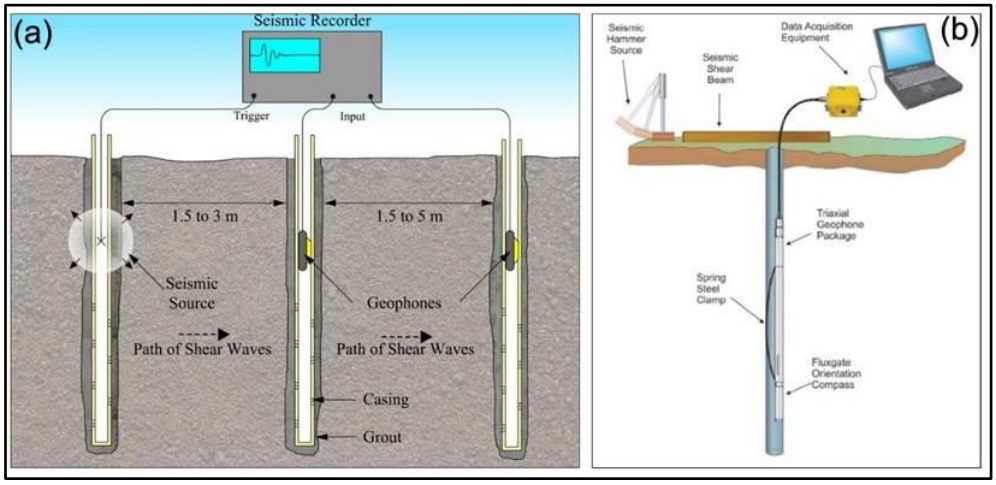

Fig. 1. Sketch of (a) the crosshole (CHST) with 3 boreholes seismic test (adapted from American Society for Testing and Materials ASTM-D4428); (b) Downhole (DH).

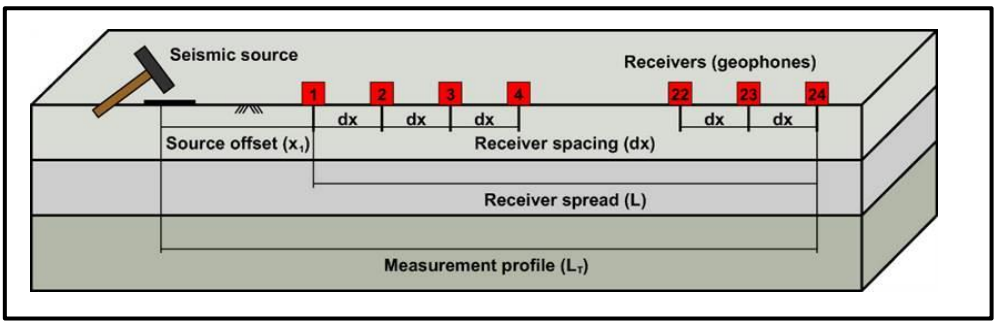

Fig. 2. MASW test procedure (Olafsdottir *et al.*, 2018)

Paper Objectives

Borehole seismic methods CHST, DHST, and MASW have been performed to delineate the geological conditions, and to estimate the elastic, dynamic soil parameters and geotechnical properties of the Al Layyah power generation plant. These objectives will be achieved based on in-situ compressional and shear wave velocities. These methods have been tested and applied for several projects all over the world by several authors (e.g., Kim *et al.,* 2004; Dietrich and Tronicke, 2009; Foti *et al.*, 2011; Al-Nuaiemy *et al.,* 2018; Al-Heety *et al.,* 2021; Al-Heety *et al.*, 2022; Baban *et al.*, 2022).

Location, Topography, and Geological Setting

The United Arab Emirates has sandy plains, mostly arid and characterized by dunes, rock mountains, valleys, and salt plains. The salt plain (called sabkha) is in the west, and the Hajar Mountains are in the east, bordering the country with Oman. Sharjah Emirate, the third largest emirate, is in between the coordinates 25° 26' 0" N and 55° 23' 0" E, with access to the west coast and east coast. It has flat, plain lands in between the coasts. The land is sandy without any vegetation. According to topographic survey, the ground level in the project region is between +3 and +4 m above the mean sea level (MSL).

The geology of the UAE has been affected by the deposition of marine sediments related to several sea-level fluctuations during geological time. The near-surface geology is dominated by Quaternary to late Pleistocene age, Aeolian dunes and sabkha deposits (Poulos, 2018). The top deposits of Sharjah City involve Quaternary "fluvial-aeolian" and shallow marine deposits. The influence of human activities has caused in the extensive deposition of man-made fill, which spreads widely in the Sharjah. The Quaternary top deposits are underlain by sandstone, siltstone, and conglomerate of the Barzaman Formation (Price *et al.*, 2012).

The survey site is flat and characterized by man-made fill deposits such as silty to silty gravelly to sand. The water level is located at 2–2.5 m below the ground surface. Generally, the main lithology from all available borehole data at the site is a very dense, slightly silty, fine- to medium-cemented sand, fine- to medium-grained calcareous sandstone, which covers only slight breaks of sand up to 25 meters deep. Table (1) shows the general stratigraphy of the project site.

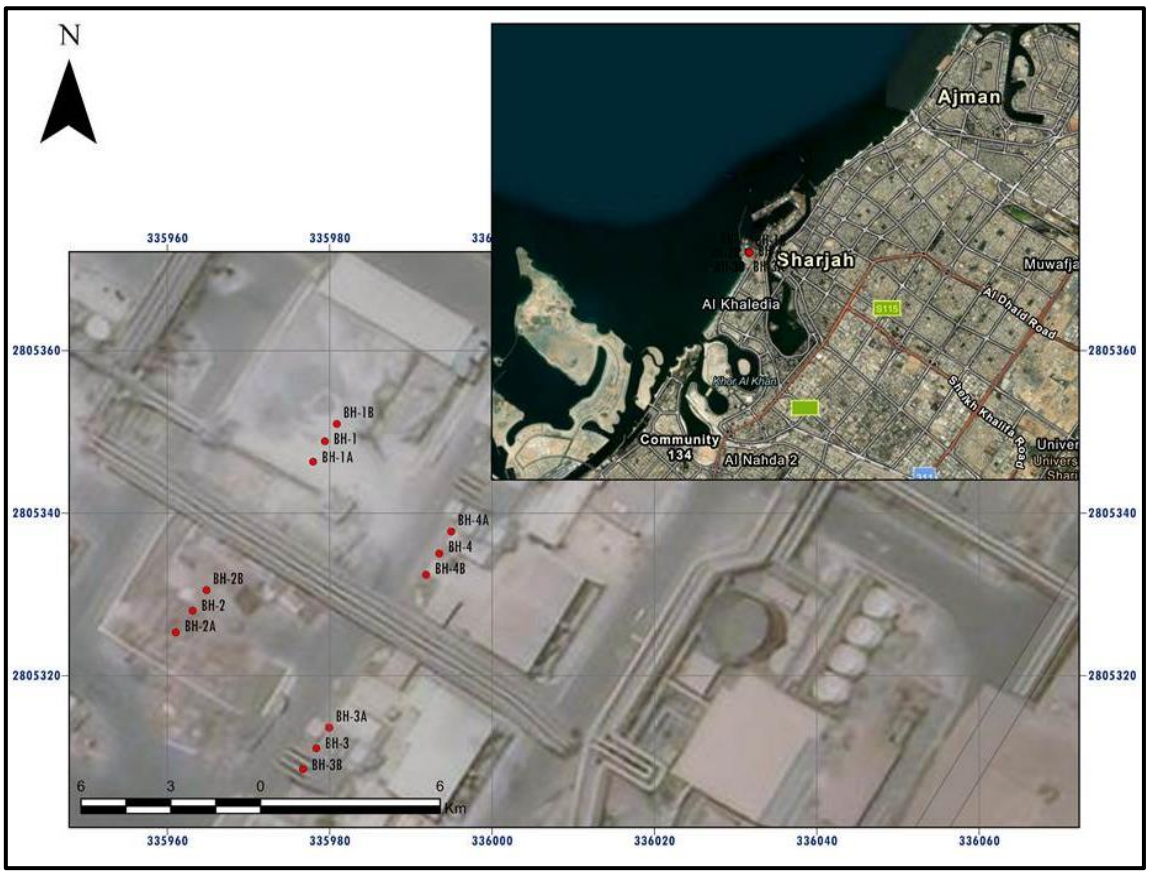

Fig. 3. Satellite Images showing the location of the borehole's seismic measurements.

Seismicity of the Study area

Over the past decade, a total of 424 earthquakes with a magnitude of four or higher have occurred within a 300-kilometer radius of Sharjah (www.earthquakelist.org). This averages out to approximately 42 earthquakes each year or about 3 earthquakes per month. On average, Sharjah experiences an earthquake roughly every 8 days. The year of 2022 witnessed a relatively high frequency of earthquakes near Sharjah, with a total of 133 earthquakes (magnitude 4 and above) recorded within a 300-kilometer range. The most powerful earthquake in that year had a magnitude of 6.0. Over the given period, 384 earthquakes, accounting for approximately 90.57% of the total, had magnitudes ranging from 4.0 to 5.0. Additionally, there were 36 earthquakes, representing about 8.49% of the total, with magnitudes between 5.0 and 6.0. Four earthquakes, making up around 0.94% of the total, had magnitudes falling within the range of 6.0 to 7.0. Notably, there were no recorded earthquakes with a magnitude of 7.0 or higher in the vicinity of Sharjah during this time frame. Minor earthquakes with magnitudes below 4.0 have been excluded from this summary. The most powerful earthquake near Sharjah in the past decade occurred on November 14, 2021. This earthquake registered a magnitude of 6.4 and its epicenter was located 274 kilometers to the north-northeast of Sharjah, at a depth of 10 kilometers. Looking further back, a significant earthquake with a magnitude of 6.9, struck on March 22, 1977, situated 271 kilometers north-northeast of Sharjah. This earthquake holds the distinction of being the most powerful seismic event near Sharjah since 1900 according to the National Earthquake Information Center, US Geological Survey (USGS-NEIC), and International Seismological Center (ISC). Figure (4a) illustrates the annual count of earthquakes within 300 kilometers of Sharjah, each with a magnitude of 4.0 or higher. Meanwhile, Figure (4b) provides the locations of the most significant earthquakes in the Sharjah region, United Arab Emirates.

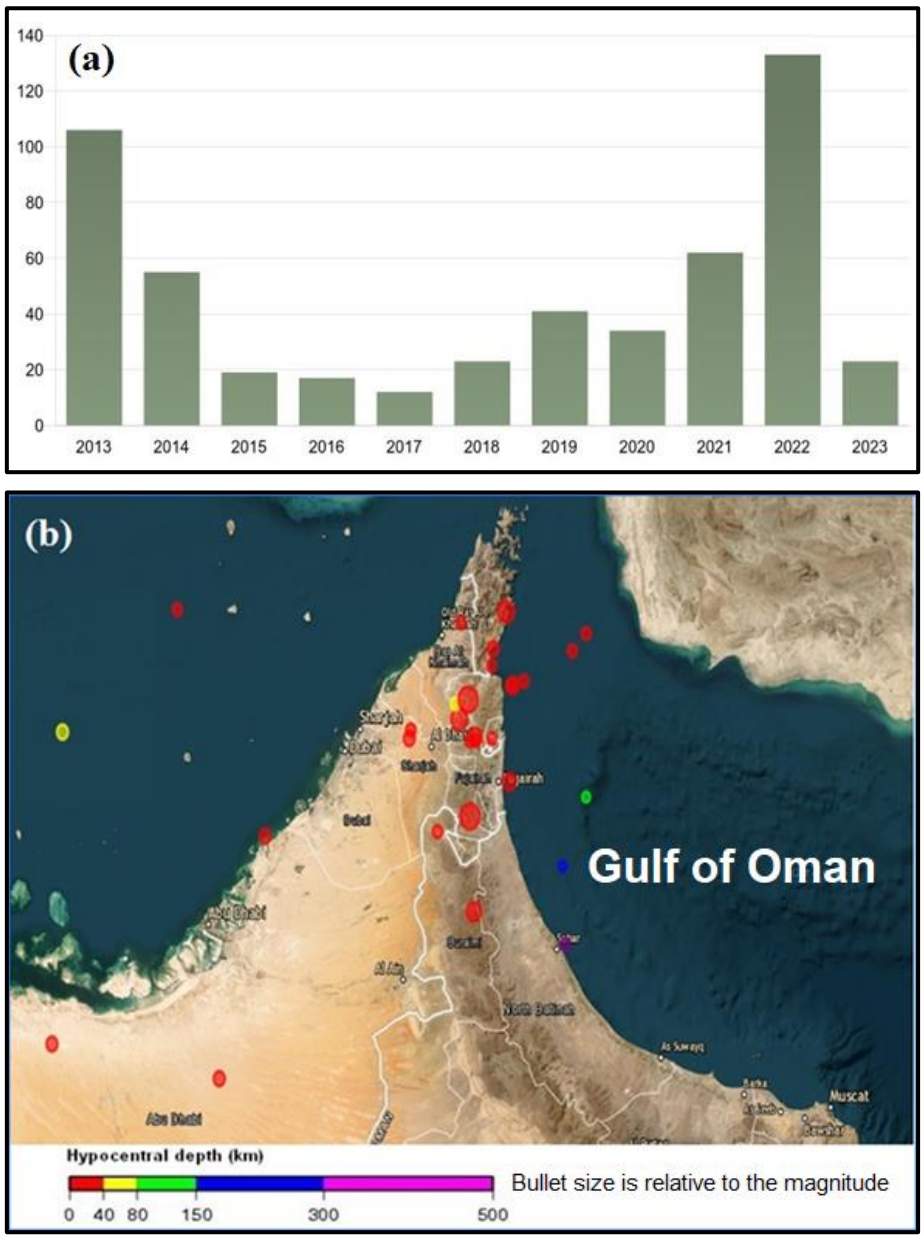

Fig. 4. (a) The annual count of earthquakes within 300 kilometers of Sharjah (https://earthquakelist.org/united-arab-emirates/sharjah/sharjah), (x-years; y- earthquakes numbers). (b) The locations of the most significant earthquakes in the Sharjah region, United Arab Emirates (UAE).

Table 1: General site stratigraphy of the project site from available boreholes.

Depth (m)	Description
0.0 m to 0.5 m	Silty to gravelly, fine to medium SAND. (MAN-MADE-FILL)
0.5m to 1.5 m	Medium dense, slightly silty to silty, very shelly, slightly gravelly, fine to medium SAND (MAN MADE-FILL).
1.5m to 5.0m	Loose to medium dense, slightly silty to silty, gravelly, fine to medium SAND (MAN MADE-FILL).
5.0m to 12.0m	Medium dense to dense becoming very dense, very shelly, gravelly, fine to medium, fine to medium SAND
12.0m to 12.2/13.32m	Very dense, very shelly, gravelly, fine to medium, fine to medium SAND with occasional cemented sand pieces
12.2/13.32m to 15.4m	Medium bedded, fine to coarse-grained CALCARENITE, slightly weathered, medium spaced, sub-horizontal to inclined fracture.
15.4 to 30.0m	Thinly bedded and laminated, locally fragmented, fine to medium-grained calcareous SANDSTONE,

Materials and Methods

Crosshole Seismic Test (CHST)

The crosshole seismic test (CHST) is often regarded as the most reliable seismic destructive method since the records are made periodically at any given depth. Since invasive methods are based on local measurements made at various depths. This technique entails pulling a source down a nearby borehole, igniting the source at a fixed depth interval, and dropping a 3-component borehole receiver down one hole. Geotechnical engineers can greatly benefit from using CHST to estimate in situ Vp and Vs with depth and the accompanying elastic soil characteristics. During CHST, body waves are only produced in the source borehole; surface waves are not, and as a result, they do not interfere with the signals of recorded body wave signals. When CHST occurs, shear waves are produced that either have horizontal (SH-wave) or vertical (SV-wave) particle movements. As an alternative, CHST can produce and record SH waves.

The fundamental of CHST techniques is the measurement of the compressional- or shear-wave travel time between the source and one or more receivers that are positioned in various boreholes at the same depth and are spaced a certain distance apart (ASTM D4428/D4428M-14). The ratio of the distance to the travel-time is then used to calculate the seismic velocity. It is possible to precisely estimate journey times with high-quality signals. The error is typically a delay in the source's activation, which causes an overestimation of travel time and, as a result, an overestimation of velocity. When a two-borehole design is used, measurements are affected by this kind of inaccuracy. When three boreholes are used, any triggering mistake is eliminated since the trip time is calculated as the difference between the travel times at the nearest and farthest receivers. According to ASTM standards, the three-borehole configuration is favored for this reason. Three estimations of the wave-propagation velocities can be taken into consideration if three boreholes are available, as shown in Figure (1):

1. The distance between the source and the initial receivers (Rx1);
2. CHST-long: the distance between the second receiver and the source (Rx2);
3. CHST: Inter-receiver path. Given that the evaluation (Rx1-Rx2) does not consider the trigger time, this number is often regarded as the most trustworthy result.

A CHST survey is conducted in April 2022 at eight borehole sites (3x8) to measure both (Vp) and (Vs). The CHST is conducted within a set of three boreholes. The location of the investigated sites is shown in Figure (3). Three installed boreholes were cased using polyvinyl chloride (PVC) casing pipe and grouted into place at each site test location to guarantee good coupling to the medium. Following the ASTM procedures (D4428/D4428M-91) to the base of the borehole, cross-hole measurements are made between three boreholes with the source and receivers at the same depth and at intervals of one meter. The depth of most of the drilling is 25 m. The elastic waves are generated at a known depth within a borehole, and the arrival times of the seismic energy are measured within a receiver borehole. From this, it is possible to determine the arrival times of the elastic waves that have traveled either directly or along discontinuities or interfaces between the three boreholes. The objective of the CHST is to investigate the dynamic and elastic properties of the subsurface materials in order to assist in the design of dynamically loaded foundations. The shear hammer was placed in one source borehole (S) and the two geophones (R) in the second and third boreholes at the same depth and elevation. The shear hammer was clamped to the borehole wall by a pneumatic clamping system (inflatable bladder). The bladder was inflated by applying air pressure through an air pump kept outside the borehole at the surface.

Down-Hole Seismic Test (DHST)

In the DHST, the source is turned on at ground level while one or more geophones are situated in a borehole. There are standards (ASTM D7400-14) that can be used for the test's execution and analysis. ASTM defines DHST as test procedures that examine waves of compression (P) and shear (S) that are traveling downward in a nearly vertical plane. For a downward propagating compression wave, the waves can be indicated as P_V or P_Z, and for a downward propagating, horizontally polarized shear wave, S_{VH} or S_{ZX}. An SH wave is another name for the S_{VH} or S_{ZX}. These tests are applied to calculate the interval velocities from the arrival times of compression (P), vertically (SV), and horizontally (SH) polarized shear waves that are produced close to the surface and descended to a number of seismic receivers that are installed vertically. A suggested technique is presented that is designed to acquire data for use on important projects where the highest quality data is required.

To produce high-quality P, SV, or both SH source waves, a variety of technologies are available. You can also use a variety of receiver and recording system options to carry out a respectable downhole survey. The configuration and type of receivers employed should deserve special consideration (ASTM, 2018). A seismic source is located at the surface, and a seismic receiver is located at some depth within the borehole. Survey recordings of downhole travel times were made at 1-meter intervals.

The data are recorded on a Geometric Geode 24-channel seismograph. The seismic wave arrivals are received using a Model BHG-4 slim hole tri-axial geophone transducer manufactured by Geostuff of Saratoga. This seismic receiver assembly houses one vertical and two horizontal 14-Hz velocity geophones in an x-y-z configuration. The transducer uses a motor-driven steel spring clamp to lock the sensors in position at each recording level in the borehole. The horizontal geophones can be oriented using a compass and servomechanism in the BHG-4 to align one of the sensors parallel to the source. Only that parallel component is recorded for the shear wave arrival. The P-wave energy source consists of vertical sledgehammer impacts on an aluminum striker plate placed on the earth surface near the borehole. The Shear-wave energy source consists of sequential sledgehammer impacts to alternate ends of a horizontal wooden beam with steel end caps. Triggering of the seismograph at the time of impact is accomplished by attaching a Geometrics impact switch to the sledgehammer. The P-wave striker plate and the S-wave impulse beam were offset from the borehole by a distance of 1.5 to 2 m to minimize coupling of the seismic energy with the borehole casing, as well as to ensure that the travel path of the seismic energy is predominantly through soils undisturbed by the borehole preparation.

Multichannel Analysis of Surface Waves (MASW)

Since the surface-wave (SW) approaches are time- and cost-effective as well as adaptable to a range of ground conditions, (SW) approaches have obtained a guarantee results for the evaluation of the shear wave velocity (Vs) model (Socco *et al.,* 2010). Many authors have compared surface wave analysis results with borehole tests since the early 2000s, when SW methods started to gain acceptance in near-surface geophysics and geotechnical engineering, to confirm the reliability of this method (e.g., Liu, 2000; Xia *et al.,* 2000; Xia *et al.,* 2002a; Stephenson, 2005; Kumar *et al.,* 2023). One of the simplest and most affordable techniques for determining shear-wave velocity is the MASW non-intrusive geophysical method. The fundamental drawback of active MASW is that its maximal depth of penetration is frequently constrained by its spread. Rayleigh wave propagation is used by the MASW method to create the Vs depth profile. Surface wave measurements are performed utilizing a set of 24 or more low-frequency (4.5 Hz) geophones that are typically spaced apart by 2 meters. A 1D versus 2D profile is created using the processed and transformed MASW data (Park *et al.,* 1999). The Rayleigh waves from the field recordings underwent processing that included figuring out the phase velocity for each frequency. The computed phase velocities for each seismic shot point at each location are summed, and the dispersion curve is produced by selecting the lowest

calculated phase velocity for each frequency component. After applying least squares inversion techniques (Park *et al.,* 1999; Xia *et al.,* 2002b) to invert the resulting dispersion curve, a Vs profile is created

The MASW test includes four main elements (Miller *et al.,* 1999). Recording shot gathers; dispersion imaging (also known as Overtone); dispersion curve (DC) estimations (from each record) (Park *et al.,* 1998); Xia *et al.,* 2007; Luo *et al.,* 2009); and then inverted DCs to acquire a 1D Vs-depth profile for each record (Xia *et al.,* 1999); for 2D image, we must gather 1D Vs-depth profiles using interpolation algorithms (Miller *et al.,* 1999). It examines the dispersion characteristics of specific seismic surface wave types (fundamental-mode Rayleigh waves) that travel from the impact point to the geophones along the surface of the measurement. The Vs (or stiffness) gives information in either the 1D Vs or 2D Vs sections.

The active MASW data have been got along one MASW line with a total length of 40 m. The measurements have been carried out between boreholes (BH-03 and BH-04) along the asphalt road at the study site. The seismic energy source for the MASW measurements is a 14-kg sledgehammer dropped on a metal plate. The survey is performed using a GEODE (Geometrics Seismograph) coupled to 24 vertical geophones with a frequency of 4.5 Hz and receiver spacing of 1 m along the lines. The projected profile length is followed while using the Standard roll-along (SRA) acquisition approach, with a source offset (X1 = -10m) for each spread and the whole spread moving forward four meters to the next location. For each shooting point, five to ten hammer strikes are used to improve the S/N ratio. The recording time is 1 second, with 0.5 millisecond sample intervals. The MASW data acquisition parameters are listed in Table (2). A summary of the geophysical and geotechnical tests conducted in the study area are shown in Table (3).

Table 2: Summarized of the (Active MASW) data acquisition Parameters.

Parameter	Setting
Acquisition System	Geode Seismograph 24 Channel
Source	Sledgehammer (14Kg)
Geophones	4.5 Hz (Land streamer with 24 take out).
Number of Geophones (N)	24
Geophones Array	Linear (roll along)
Geophones Spacing (dx)	1 m
Array Dimension (D)	23 m
Source Offset (X1)	10 m
Source –Receiver move (dSR)	4 m
Shallowest depth of investigation (Z min)	1 m
Sample interval (dt)	0.5 milliseconds
Record length (L)	1 second

Table 3: Summary of the tests performed in the study area.

Test type	Number
Borehole	24
Standard Penetration Test (SPT)	4
Cross-Hole (CHST)	8
Down-Hole (DHST)	1
MASW line Between BH-03 and BH-04	1

DATA PROCESSING

CHST and DHST Data

To avoid the not reflective data of the subsurface nature, processing CHST and DHST data requires QA/QC procedures. This procedure is crucial when the data S/N ratio is low. The first step is to display the first arrival times picking of both wave types (Vp and Vs) for each recorded signal. Figure (5 a) plot shows primary- and shear-wave from impulse and reversible impulse seismic sources for DHST and CHST, respectively (ASTM, 2018 and 2014). The seismic arrival times are limited by picking the first-arrivals of the seismic data (waveforms)

interactively using a powerful processing tool and the interactive SeisImager suite (Geometrics Inc., San Jose, CA) for obtaining the Vp and Vs of materials at concern depths from seismic records. The raw seismic data are loaded into the processing program. Processing raw data in the first stage entail editing seismic records and using frequency filters to improve the first arrival time. Figure (6) shows two examples of seismic data after applying filtering. The first arrivals of primary and shear waves are selected during the second phase, which came after the amplification of the recorded signals. By choosing the time at which every geophone component recorded the first coherent energy, an accurate automatic picker with manual override is able to immediately identify the first arrivals. Picking first arrivals from CHST and DHST data requires estimating first break positions based on one's own perceptions, which can be challenging at deeper receiver depths where the SNR is low. The arrival times are converted from the slant-path arrival times to vertical-path arrival times by multiplying by the cosine of the angle formed by the wellbore and the slant path of the seismic wave. Vertical travel-time curves are then constructed using this corrected data. Finally, a best-fit velocity is selected for each linear segment of the primary- and shear-waves travel-time curve, providing representative Vp and Vs distributions down the borehole.

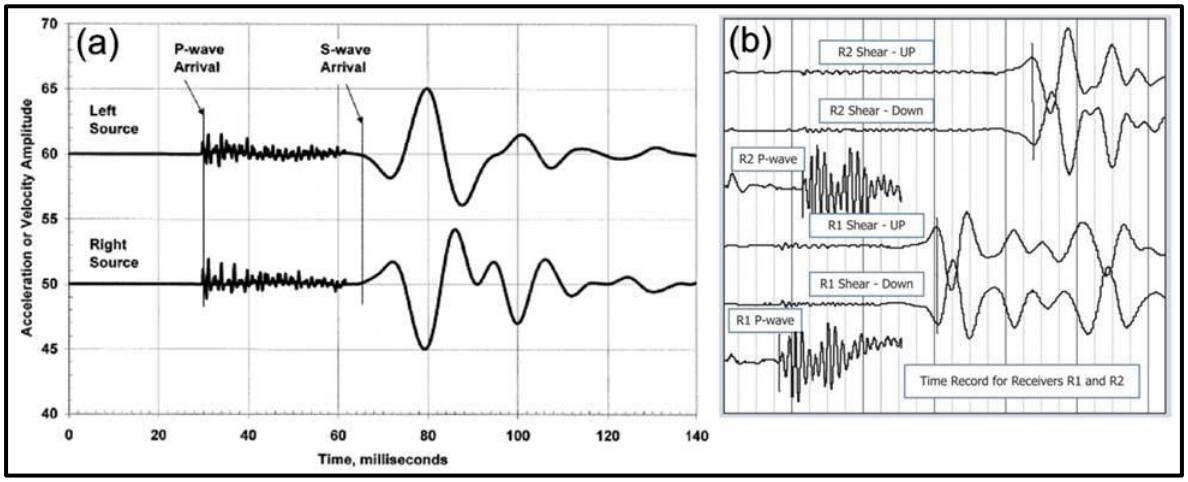

Fig. 5. A plot showing (P- and S-Wave) from (a) Impulse seismic source for DHST; (b) Reversible impulse seismic source for CHST (ASTM, 2018 and 2014).

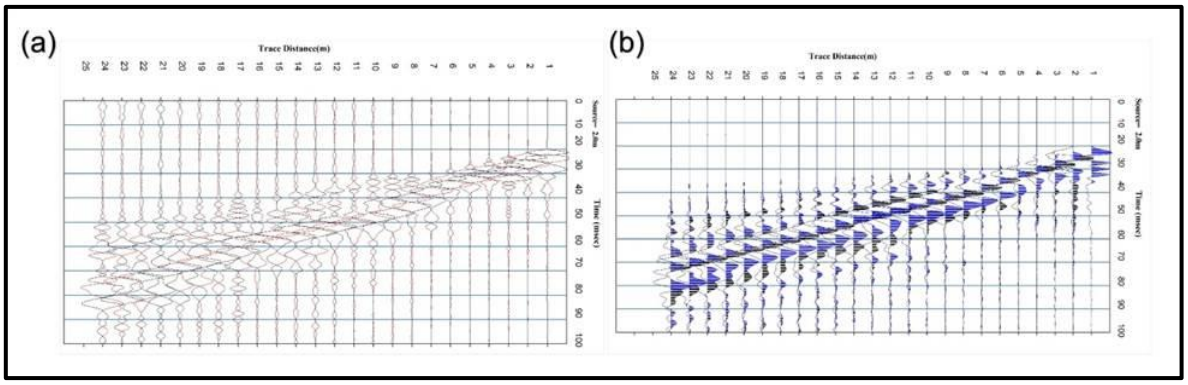

Fig. 6. Two examples of CHST seismic data (a) and (b) after applied filtering to enhance data for the first break phase.

MASW Data

MASW, by interpolating the collected 1D Vs-depth models in a successive order depending on the receiving station, a SurfSeis software is used to analyze the data and create 2D Vs pseudo-sections. The phase-shift method (Park *et al.,* 1998), a 2-D wavefield transformation that can be remapped from the *f-k* transform (Ivanov *et al.,* 2015) is used to image the dispersion properties. Each multichannel record is transformed into a dispersion-curve image, after which the required dispersion features (fundamental mode) can be realized

and assessed with a certain energy trend. The DC file is generated from the picked points and then inverted to provide 1D Vs-Vs profiles for each seismic record. The mapping together with several 1D vs. depth profiles produce 2D vs. cross-sections (Miller *et al.,* 1999). The accurate calculation of the DC is the most significant factor controlling the accuracy of the Vs profile since the 2D Vs pseudo sections are based on the inversion of DCs. The final 2D V-section had a low "Root Mean Square Error (RMSE)", which revealed good confidence (Xia *et al.,* 1999). Figure (7) shows the procedure to produce a 2D or pseudosection.

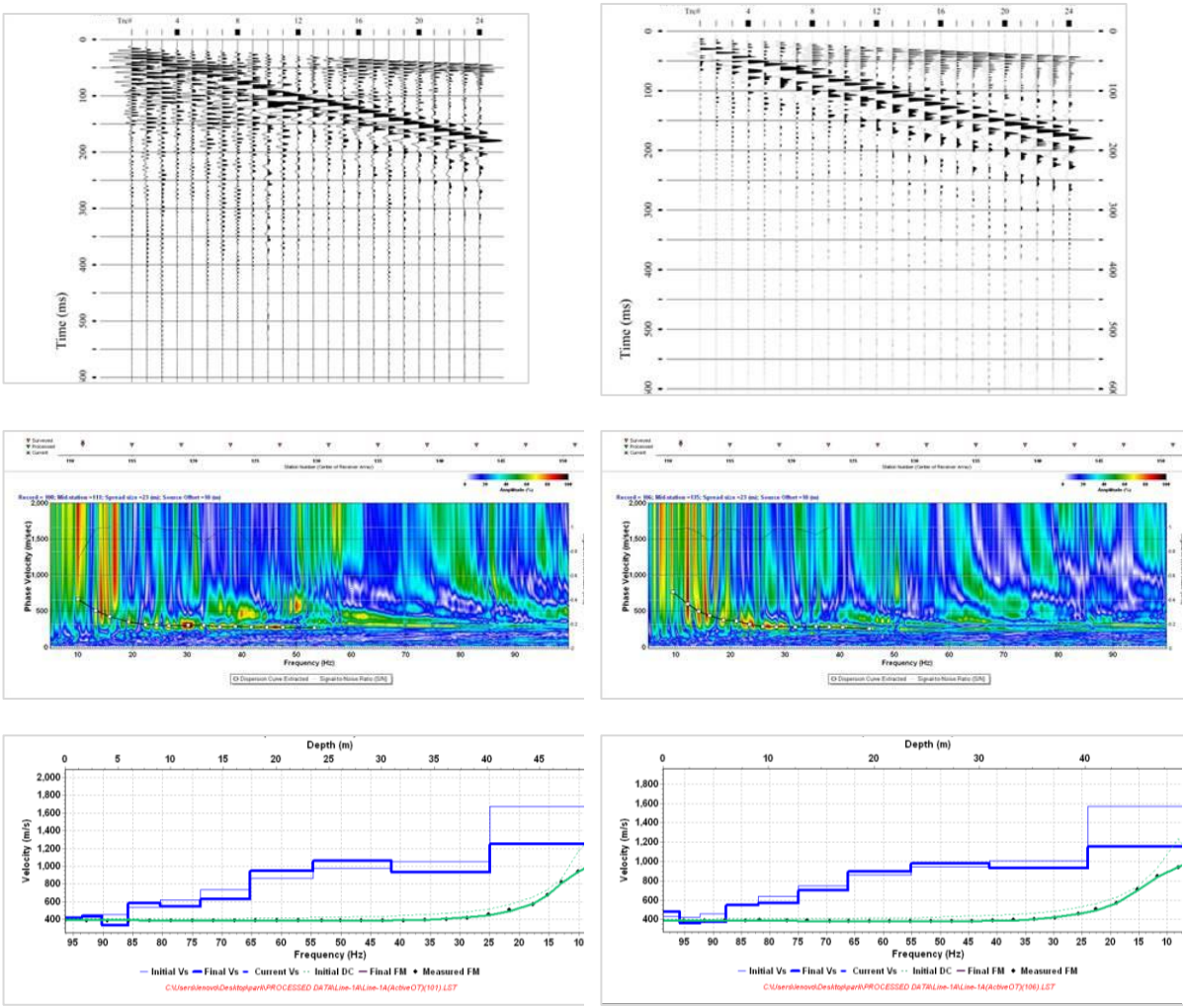

Fig. 7. Raw shot gathers, dispersion-image, and the picked DCs, inverted 1D Vs-depth profile of MASW line (SP-101, 106).

Results and Discussion

CHST and DHST

The first arrivals found on the trace by hand picking are used to calculate the compressional and shear-wave travel time using *Pickwin* software for every shot-receiver location and used with the identified offset (s) between the shot and receiver depth or successive records (1 m) to calculate the Vp and Vs for every depth interval.

The SH-wave signals from the regular and reverse source pulses should ideally be almost mirror reflections of one another. Although different waveform locations are used if the first pulse is distorted, the first maxima are chosen for the normal signals and the first minima are chosen for the reverse signals. The seismic velocity results from CHST from the surveys at three locations (BH-1, BH-3, and BH-4) are presented via Origin Pro (Origin Lab) software in Figure (8), while DHST is presented in Figure (9). These figures also show elastic modules and Poisson's ratio, which are plotted against depth. The profiles of the CHST and DHST velocities

and elastic modules for BH-4 are plotted against depth and lithological log in Figure (10). The borehole log shows the stratigraphic subdivision of the strata. Tables (4 and 5) summarize the CHST and DHST results at BH-04 (Vs, Vp, and estimation of engineering parameters). Table (6) summarizes the soil/rock strata and calculates the density (ρ).

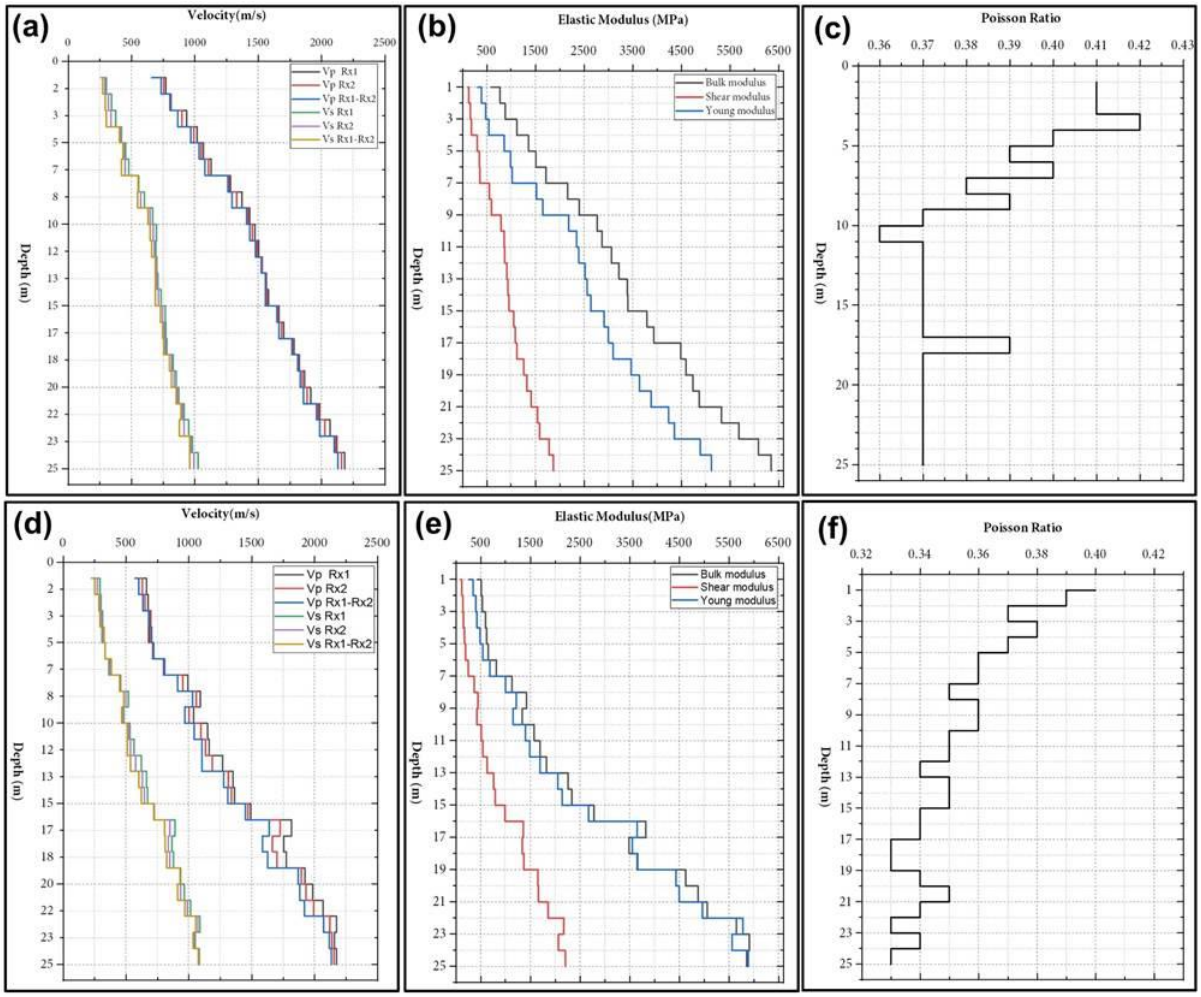

Fig. 8. Graph of Crosshole at BH-01 seismic result (a) Vs, Vp; (b) Elastic modulus and (c) Passion's ratio; and (d-e-f) at BH-3 location.

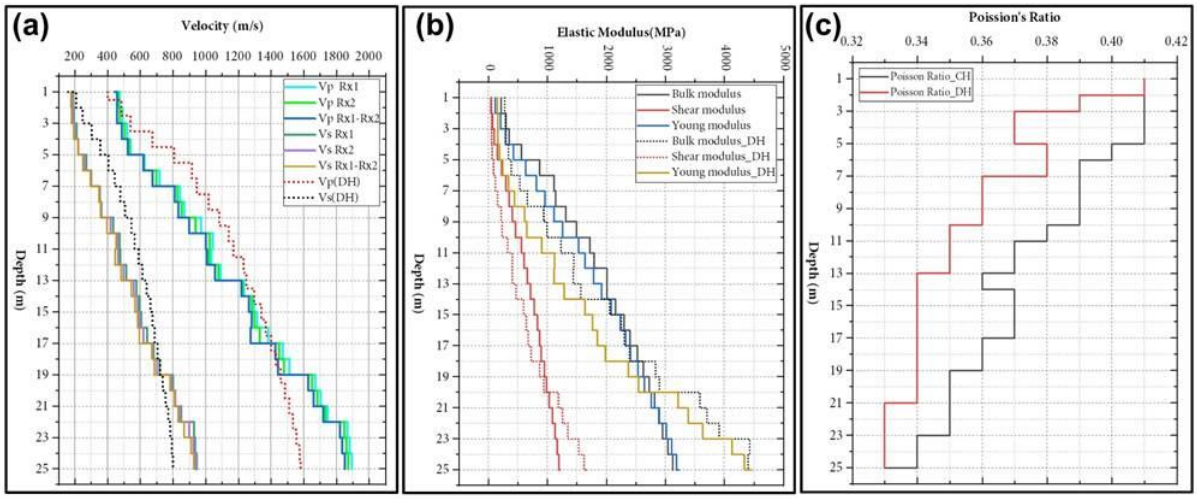

Fig. 9. Graph of CHST and DHST at BH-04 seismic result: Vs, Vp; elastic Modulus and (c) Passion's ratio.

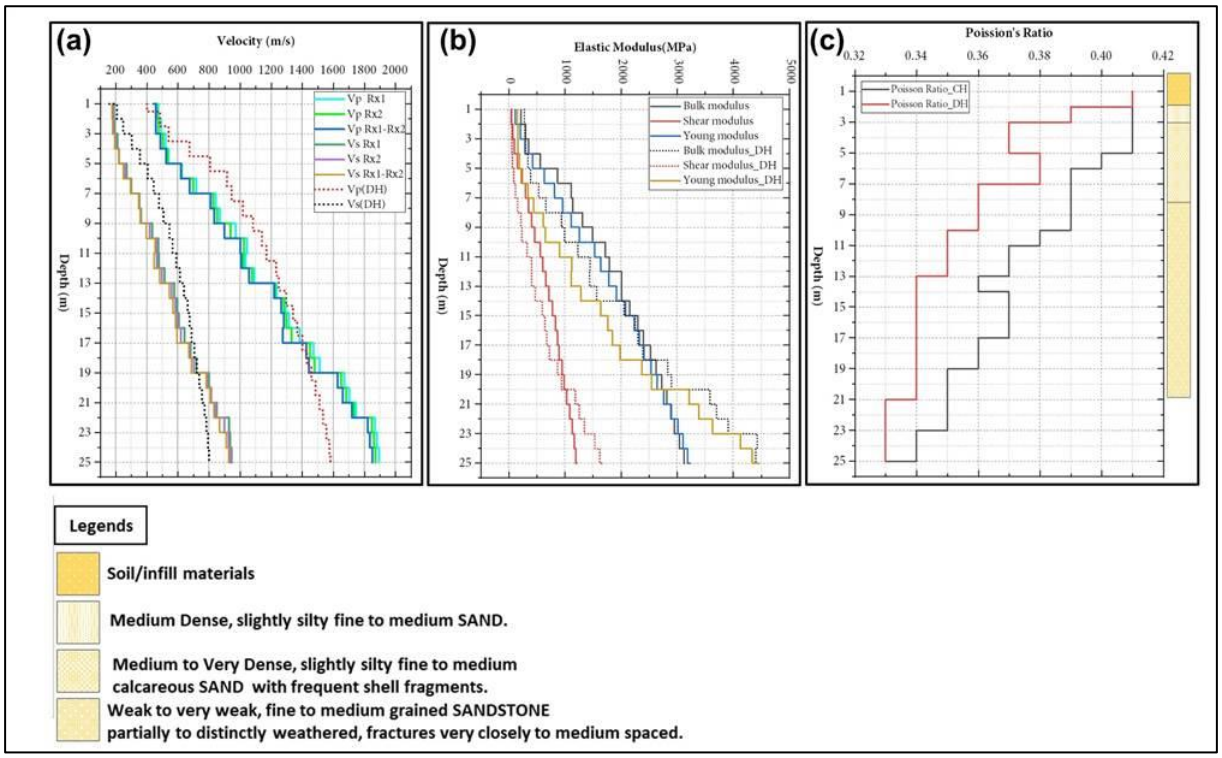

Fig. 10. Graph of CHST and DHST @BH-04 seismic result: Vs, Vp; elastic Modulus and (c) Passion's ratio.

MASW

A MASW profile of length 40 m has been carried out between BH-03 and BH-04 along the asphalt road. The final MASW results are represented by 2D (Vp) and (Vs) sections. From MASW results, the Standard Penetration Test (SPT), Poisson's Ratio, and shear modulus map are generated as shown in Figure (11). To illustrate the relative range in velocity values and other features, a rainbow color scheme is utilized. The outcome high-resolution 2D images display the sub-surface characteristics discovered reaching to around 30 meters of depth, including soft layers with variable degrees of compactness and rock components with varying elastic capabilities and rigidity. Four stratigraphy beds are obviously recognized: a low Vs bed (white and blue), underlain by a rather high Vs (green), underlain by high Vs (yellow and red).

It can be seen that the shear wave velocity of the top bed is very low, less than 200 m/s indicating a low compaction. The depth of this bed is between 0.5 and 2 meters. This bed is typical of very loose soil fill materials, which are observed to characterize the topsoil. The second layer is low ranging between 200 and 450 m/s and indicating a modest compaction. The depth of this layer is between 2 and 10 meters. This layer is typical of dense soil, which is observed to characterize the sand. The second layer has Vs ranging between 450 and 800 m/s and corresponds to stiff soil materials or soft rock. The depth of this layer is between 10 and 20 meters. However, particular anomalies (low velocity) are noticed in the middle of the MASW profile (from 15 to 25 m in distance). The deeper layer below 25 m seems to be more compacted, with Vs increasing with depth (Vs > 800 m/s) corresponding to less weathered rock formation. The high values of Vs (above 800 m/s and 1000 m/s, respectively) suggest that the rock is competent. These velocities point to the presence of soil and rock components, such as sand and sandstone. There are no obvious low-velocity zones under the high-velocity zones that may be considered cavities or quiet dangerous zones. According to the Vs section, and as a result, there are no potential hazards that could raise suspicion or dread before beginning construction operations throughout the studied region. However, weak sandstone is indicated by a thin, weak layer or zone that is visible at depths between 12 and 15 meters. The geotechnical findings from the BH-03 and/or BH-4 boreholes, which are crucial in supporting the MASW data, show that the study area's SPT N value supports medium- to dense-density soil (SPT-N values varying

from 10 to >50). In any of the drilled boreholes in the research area (with depths of 25 m), no cavities are found. In all of the drilled boreholes, the groundwater level is found between 2 and 2.5 m. It is necessary to correlate the MASW and geotechnical results (Fig. 8) in order to fully evaluate the study's data and to support the geophysical conclusions using ground techniques (e.g., borehole drilling). Figure (8) shows an interpreted section that correlated the results from the drilling log of BH-03 (20 m depth) and the Vs of the MASW line (20 m depth) versus the recovered core samples. There is a MASW line between BH-03 and BH-04. The 2D section shows a stratification indicating a series of rising Vs versus depth to around 30 m demonstrating a high correlation between the outcomes of both datasets. The following geological model might be offered depending on this combined analysis of MASW and geotechnical results **(**Fig. 8):

1. Layer 1: soil/infill materials, with a thickness of 2 m and a Vs of 200 m/s.
2. Layer 2: medium dense, calcareous, fine sand with occasional shell fragments, slightly silty with a Vs of 200–450 m/s and a thickness of 2–10 m. Very dense, somewhat silty, finely cemented SAND makes up the majority of the lower 9 to 12 meters of this layer. And the SPT "N-values" under this depth and through the end of this unit are > 50; those discovered at the top 2.0–4.0 m varying between 28 and 16, and those encountered at 4.4–11 m range between 10 and 26.
3. Layer 3: fractures are very tightly spaced to moderately spaced, and the SANDSTONE is weak to very weak, with a fine to medium-grained thickness of 12 m or less and a Vs range of 450–800 m/s. It consists of extremely weak stone that is brown, somewhat to moderately worn, and fractured. Total core recovery (TCR) values for the SANDSTONE layer extend from 76% to 100%, and rock quality designation (RQD) values are between 13% and 30%, with some levels of extensive fracturing resulting in zero RQD and TCR values. 100 SPT N-values are encountered, counting from top to bottom.
4. Layer 4: possibly exceedingly hard, thick SANDSTONE (based on MASW): a shear wave velocity of 800-1200 m/s and a thickness of approximately 14.0 m. This layer's interpretation often matches the accepted conventions and expectations. Lithology consists of sand interbedded with gypsiferous sandstone.

Furthermore, the dynamic properties, e.g., the SPT value and shear modulus maps, are estimated from the MASW section. The conversion of the Vs section to SPTN (empirical method) coefficients, 78 and 0.4, are from Anbazhagan and Sitharam (2008). The shear modulus is obtained from the square of Vs; hence, it is sensitive to velocity changes.

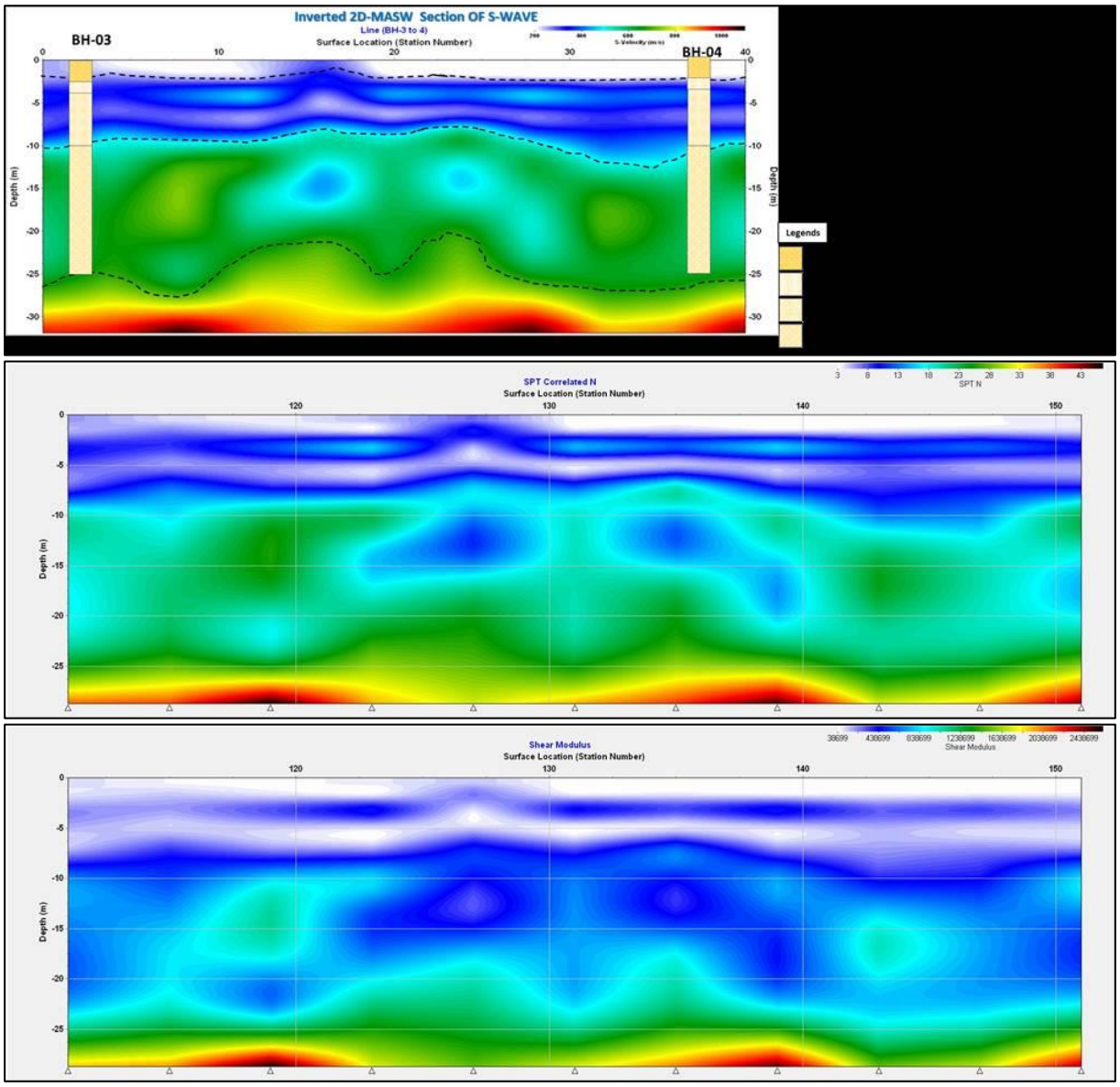

Fig. 11. 2D MASW section between BH-03 and BH-04 reveal the vertical and lateral change of the Vs; SPT values; and shear modulus (unit: Mpa) derived from MASW results by *SurfSeis* software respectively.

A Comparison of CHST, DHST and MASW Vs profiles results

Crosshole seismic test (CHST), downhole seismic test (DHST), and MASW are assessed based on of shear wave velocities at BH-3 and BH-4 test sites as presented in Figure (12). It is worth mentioning that the active MASW line is acquired between boreholes BH-03 and BH-04 along the asphaltic road with a total length of 40 m at the study site. CHST is mostly considered to be more consistent and precise than MASW for various reasons; first, in the CHST method, travel times and travel offsets are determined straight-forward and used to calculate Vs. In contrast, the MASW method measures phase-dependent surface wave velocities and uses these to estimate Vs as a function of depth; second, MASW Vs denote average velocities through lateral offsets, typically of 30 m; and third, MASW Vs represent “average velocities” across depth intervals that increase with depth of burial. The differences between the CHST, DHST, and MASW vs. 1D profiles may be attributed to the fact that MASW velocities are averaged vertically and laterally. All of the derived profiles are fairly similar.

The largest discrepancy in Figure (12) is evident at two zones: zone one is between 2 and 4 m, and zone two is between 9 and 13 m deep, where MASW results yield a higher estimation of the Vs value than CHST. The boundary between zone one and zone two is a dense, silty sand

and a medium dense, silty calcareous sand. The top of a very dense sand layer with > 50 SPT N-value is found in zone two but not in detail by the MASW analysis. However, the other features of MASW make it a better choice than CHST and DHST for general soil categorization to depths of 30 m. MASW data is also less expensive than borehole seismic testing and can typically be obtained in locations inaccessible to drill rigs. Another significant advantage of the MASW tool over borehole seismic tools is its ability to map varied depths to bedrock (Anderson *et al.,* 2007). This leads to a relatively high soil impedance, making the interpretation of test results problematic in cases of CHST, DHST, and MASW. However, computed Vs30 values for MASW are 483 m/s and 462 m/s for borehole seismic tests (4% difference). In most categorization systems, the difference in Vs30 values does not modify the soil type (Dobry *et al.,* 2000). The outcomes are typically close together. MASW results are generally equivalent to CHST and DHST data but significantly less precise and dependable. Boreholes BH-3 and BH-4 encounter bedrock at a depth of about 20 meters. Data for CHST and DHST at BH-4 are achieved at a depth of 25 m.

MASW control covers a depth of around 30 m at the borehole seismic test location. The BH-3 CHST-Vs profile is believed to be more precise than the MASW 1D Vs-depth profiles. The visual assessment of the CHST profile shows that the Vs of soil gradually increases with depth (from 235 m/s to 650 m/s at a depth of 15 m). The soil of BH-3 is almost entirely made up of sand, silt, and sandstone. Slight variations in lithology are responsible for the observed slight oscillations in Vs. The BH-4 CHST and DHST-Vs profiles are likewise thought to be more accurate than the MASW-1D profiles. Visual inspection of the CHST and DHST profiles reveals that the Vs of soil steadily rises with depth (from 180 m/s (CHST) and 160 m/s (DH) to 580 m/s (CHST) and 660 m/s (DHST) at a depth of 25 m). The soil of BH-3 is mostly made up of sand, silt, and clay. The MASW 1D Vs profile is similar to the CHST profile at BH-3, with the exception that MASW shear wave velocity values are constantly equal to, slightly less than, or slightly greater than the corresponding CHST values. MASW velocities range from about 250 m/s to approximately 610 m/s (at a depth of 15 m), whereas CHST Vs values range from approximately 235 m/s to approximately 650 m/s. The findings of MASW and downhole tests are extremely comparable, and no change in soil classification is predicted until the Vs30 value is near the limitations for a certain seismic soil type. The derivation of shear wave velocity Vs profiles using DHST and active MASW tests is quite comparable, except in rare circumstances where there is an intermediary dense sandy-gravel layer that MASW analysis does not capture.

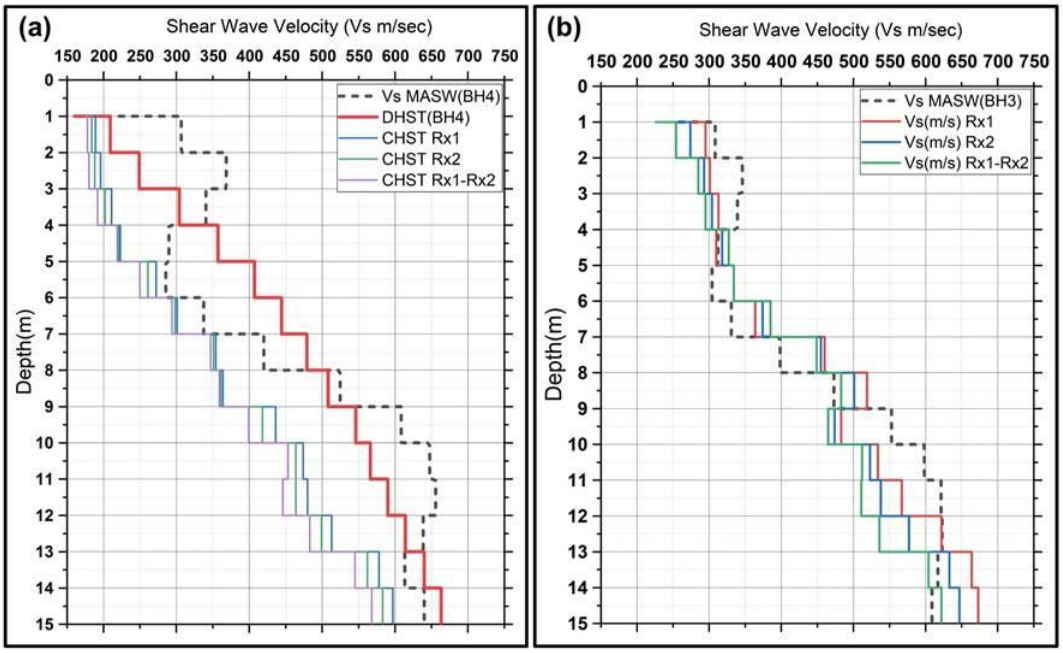

Fig. 12. CHST, DHST and MASW (1D Vs) profiles comparison (a) for test site at BH-4; (b), for test site at BH-3.

Estimation of geotechnical soil parameters

Using mean Vs and Vp values and the bulk density (ρ) as shown in Table (4), soil dynamic properties, e.g., dynamic shear modulus, Poisson's ratio, young's modulus, and bulk modulus, can be calculated using equations in Table (5) depending on the relations given. Tables (6 and 7) summarize Vs, Vp and estimation of engineering parameters from CHST and DHST results.

Table 4: Summarized soil/rock Strata and calculated density (ρ).

No.	Strata depth (m)	Strata description	density(ρ) kg/cc
1	4.0	Medium dense Sand	1.7
2	4.0- 9.5	Medium dense Sand with shell fragments	1.8
3	9.50-12.0	Very dense sand	1.9
4	12.0-25.0	Sandstone	1.9

Table 5: The relationships used for dynamic parameters estimation (modified from (Abdelrahman *et al.*, 2020; Al-Saigh and AL-Heety, 2018)

Elastic Module	Used Formula
Poisson's Ratio (δ)	$\sigma = \frac{1}{2}\left[1 - \frac{1}{(V_p/V_s)^2 - 1}\right]$
Young's Modulus (E)	$E = \rho\left[\frac{3Vp^2 - 4Vs^2}{\left(\frac{vs}{vp}\right)^2 - 1}\right]$
Shear Modulus (μ)	$\mu = \left[\frac{E}{2(1+\sigma)}\right]$
Bulk modulus (K)	$K = \frac{E}{3(1-2\sigma)}$

Table 4: CHST result from BH-04 summarized Vs, Vp, and estimation of engineering parameters.

depth (m)	density(ρ) g/cc	Vp (m/s) Rx1	Vp (m/s) Rx2	Vp (m/s) Rx1-Rx2	Vs (m/s) Rx1	Vs (m/s) Rx2	Vs (m/s) Rx1-Rx2	Bulk (MPa)	Shear (MPa)	Poisson ratio	Young (MPa)
1	1.7	468	456	443	187	181	176	278	56	0.41	157
2	1.7	475	466	457	189	183	178	293	57	0.41	161
3	1.7	491	475	459	196	188	179	304	60	0.41	168
4	1.7	521	505	489	211	202	192	342	69	0.41	194
5	1.8	540	533	525	223	221	219	394	88	0.40	246
6	1.8	628	624	619	272	261	250	537	123	0.39	342
7	1.8	720	698	675	301	298	294	665	159	0.39	443
8	1.8	844	828	811	354	351	347	939	221	0.39	616
9	1.85	871	853	833	364	361	359	996	235	0.39	653
10	1.9	974	938	901	436	418	399	1231	331	0.38	912
11	1.9	1046	1025	1002	474	464	453	1450	409	0.37	1121
12	1.9	1034	1023	1010	480	464	446	1443	408	0.37	1119
13	1.9	1092	1076	1059	513	499	483	1570	473	0.36	1289
14	1.9	1236	1227	1218	578	562	545	2061	600	0.37	1641
15	1.9	1295	1281	1265	597	583	568	2254	647	0.37	1770
16	1.9	1316	1300	1282	607	597	586	2306	677	0.37	1850
17	1.9	1383	1330	1276	642	619	596	2392	729	0.36	1984
18	1.9	1472	1450	1426	684	677	670	2833	871	0.36	2371
19	1.9	1513	1479	1443	718	704	689	2902	942	0.35	2550
20	1.9	1672	1651	1628	801	792	782	3587	1192	0.35	3220
21	1.9	1703	1683	1661	816	814	811	3706	1257	0.35	3389
22	1.9	1747	1734	1720	852	843	833	3914	1350	0.35	3632
23	1.9	1868	1847	1823	928	899	869	4431	1536	0.34	4130
24	1.9	1881	1860	1837	937	925	912	4405	1625	0.34	4342
25	1.9	1894	1873	1851	947	938	929	4438	1673	0.33	4459

Table 5: DHST results BH-04 summarized Vs, Vp and estimation of engineering parameters.

Depth (m)	density(ρ) kg/cc	Vp (m/s)	Vs (m/s)	Bulk (MPa)	Shear (MPa)	Poisson Ratio	Young's (MPa)
1.0	1.7	401	160	216	43	0.41	122
2.0	1.7	485	209	301	74	0.39	206
3.0	1.7	541	249	358	105	0.37	287
4.0	1.7	675	304	566	157	0.37	431
5.0	1.7	808	357	871	229	0.38	632
6.0	1.8	917	407	1116	298	0.38	820
7.0	1.8	947	444	1141	355	0.36	965
8.0	1.8	1019	479	1318	412	0.36	1120
9.0	1.8	1083	508	1494	465	0.36	1263
10.0	1.85	1142	546	1724	566	0.35	1532
11.0	1.9	1171	566	1794	608	0.35	1640
12.0	1.9	1233	590	2008	661	0.35	1786
13.0	1.9	1250	614	2016	716	0.34	1920
14.0	1.9	1297	640	2161	778	0.34	2083
15.0	1.9	1341	663	2304	835	0.34	2235
16.0	1.9	1368	676	2400	868	0.34	2324
17.0	1.9	1401	688	2529	899	0.34	2412
18.0	1.9	1431	707	2626	949	0.34	2540
19.0	1.9	1459	722	2727	990	0.34	2648
20.0	1.9	1486	738	2816	1034	0.34	2763
21.0	1.9	1511	756	2887	1087	0.33	2896
22.0	1.9	1534	773	2958	1134	0.33	3017
23.0	1.9	1556	784	3043	1167	0.33	3104
24.0	1.9	1576	794	3125	1197	0.33	3186
25.0	1.9	1582	801	3132	1218	0.33	3235

Soil Profile Type and (Vs-30)

According to Dubai International Building Code (DIBC 2004), the average Vs of the upper 30 m (Vs30) below the foundation is used to classify the soil profile as in Table (8). The (Vs 30 m) is calculated as follows:

$$V_s^{30} = \frac{30}{\sum_{i=1}^{N}(\mathrm{hi}/\mathrm{vi})}$$

where: hi= thickness (m), and vi= Vs_{30} (m/s).

The average S-wave and p-wave velocities in 8 crosshole and 1 downhole are shown in Table (9). The average of the upper (Vs-30) is found to be 462 m/s; therefore, the site soil profile classification is found to be of class C “Very dense soil and soft rock” according to Dubai Municipality Building Code (DIBC-2004) and International Building Code (IBC 2009).

Table 6: Soil Profile Type (According to International Building Code (IBC 2009) and Dubai International Building Code (DIBC 2004)

Site Class	Soil Profile Name	Average Properties in Top 30 m		
		Soil Vs (m/s)	Standard penetration resistance, N	Soil undrained shear strength, S m, (psf)
A	Hard rock	VS >1,500	N/A	N/A
B	Rock	750 < VS ≤ 1,500	N/A	N/A
C	Very dense soil and soft rock	360 < VS ≤ 750	N >50	Sμ ≥2,000
D	Stiff soil profile	180 ≤ VS ≤ 360	15 ≤ N ≤ 50	1,000 ≤ Sμ ≤ 2,000
E	Soft soil profile	VS ≤ 180	N < 15	Sμ < 50

Table 7: Average Vp and Vs in the study area.

Method	BH Name	Depth (m)	Average Vs (m/s)	Average Vp (m/s)
CHST	BH-1A-1-1B	25	636	1458
	BH-2A-2-2B	25	594	1284
	BH-3A-3-3B	25	617	1271
	BH-4A-4-4B	25	607	1334
	BH-5A-5-5B	10	283	644
	BH-6A-6-6B	10	291	716
	BH-7A-7-7B	10	292	678
	BH-8A-8-8B	10	271	640
DHST	BH-4	25	567	1169
Total Average			462	1021

Conclusions and recommendations

The engineering parameters have been determined based on the CHST and DHST results at BH-04. Soil dynamic properties including “dynamic shear modulus, Young's modulus, Poisson's ratio, and bulk modulus” have been calculated using mean Vs and Vp values and the bulk density. A 40-meter-long MASW profile has been created along the asphalt road between BH-03 and BH-04. Seismic sections of 2D P-wave velocity (Vp) and S-wave velocity (Vs) are used to illustrate the inversion results of the MASW survey. The Standard Penetration Test (SPT), Poisson's Ratio, and shear modulus map are produced from the MASW data. The underlying details can be seen in high-resolution 2D cross-sections that are extended down to a depth of around 30 m. These cross-sections include soft layers with varied degrees of compactness and rock materials with different elastic characteristics and stiffnesses. A low-velocity layer as shown in Figure (11) of (white and blue) color is overlaid by a comparatively high-velocity layer (green), which is then overlaid by a high-velocity layer (yellow and red). There are no obvious low-velocity zones below the high-velocity ones that may be interpreted as cavities or really hazardous zones, according to the Vs cross-sections, and as a result, there are no potential hazards that could raise suspicion or dread before beginning construction operations throughout the investigated region. However, weak sandstone is indicated by a thin, weak layer or zone that is visible at depths between 12 and 15 meters. Additionally, the MASW section is used to determine the soil's dynamic properties, like the SPT value and shear modulus maps. The soil profile type is chosen using the statistical average Vs of the top 30 meters (Vs30). This profile is thus chosen using the statistical variance of 30. According to the Dubai Municipality Building Code (DIBC-2004) and the International Building Code (IBC 2009), the site soil profile is classified as "very dense soil and soft rock” since the Vs 30 is found to be 462 m/s. Based on the results of this study, it is recommended that the integration between surface and subsurface geophysical data measurements will be of great benefits for the site soil characterization at the strategic and developmental sites.

Acknowledgments

We thank the managers of Tatweer for Geophysical Studies and Consulting (TGSC), Abu Dhabi, U.A.E. owner of the data to have let us obtained the authorizations for this work. This research is funded by the Researchers Supporting Project number RSP2023R351, King Saud University, Riyadh, Saudi Arabia.

References

Abdelrahman, K., Alamri, A. M., Al-Otaibi, N. and Fnais, M., 2020. Geotechnical assessment for the ground conditions in Makah Al-Mukarramah city, Saudi Arabia. Journal of King Saud University-Science, 32(3), 2112–2121. https://doi.org/10. 1016/j.jksus.2020.02.011

Al-Heety, A. J., 2016. Velocities Extraction Efficiency of shear Waves from Rayleigh Waves by Applying Multichannel Analysis of Surface Waves Technique and Their Relation by A Number of Geotechnical Parameters. Iraqi Bulletin of Geology and Mining, 12(2), 1-10. https://ibgm-iq.org/ibgm/index.php/ibgm/article/view/316

Al-Heety, A. J., Hassouneh, M., Abdullah, F. M., 2021. Application of MASW and ERT methods for geotechnical site characterization: A case study for roads construction and infrastructure assessment in Abu Dhabi, UAE. Journal of Applied Geophysics, 193, 104408. https://doi.org/10.1016/j.jappgeo.2021.104408

Al-Heety, A. J., Shanshal, Z. M. and Al-Mashhadany, A. Y., 2022. Application of Multi-Channel Analysis Surface Waves and Electrical Resistivity Tomography Methods to Identify Weak Zones at University of Mosul, Northern Iraq. The Iraqi Geological Journal, 47-69. https://doi.org/10.46717/igj.55.1D.4Ms-2022-04-20

Al-Nuaiemy, A. Z., Al-Juraisy, B. A. and Al-Mafraji, M. A., 2018. The Use of the Seismic Refraction Tomography Survey Method and the Multi-Channel Analysis Technique of Surface Waves in the Geotechnical Assessment of the Al-Amal Apartments Site in Kirkuk, Northern Iraq, Iraqi National Journal of Earth Science, 18(2), 89-104. (In Arabic) https://doi.org/10.33899/EARTH.2018.159260

Al-Saigh, N. H. and Al-Heety, A. J., 2013. Seismic Refraction Tomography and MASW Survey for Geotechnical Evaluation of soil for the Teaching Hospital Project at Mosul University. Journal of Zankoy Sulaimani - Part A, 16(1), 1–14. https://doi.org/10. 17656/jzs.10279

Al-Saigh, N. H. and Al-Heety, A. J., 2018. 2-D Seismic Refraction Tomography for Site Investigation of the Teaching Hospital Project at Mosul University. Iraqi National Journal of Earth Science, 18(1), 77–86 (in Arabic). https://doi.org/10.33899/earth.2018.159280

Anbazhagan, P. and Sitharam, T. G., 2008. Site characterization and site response studies using shear wave velocity. Journal of Seismology and Earthquake Engineering, 10(2), 53-67.

Anderson, N., Thitimakorn, T., Ismail, A. and Hoffman, D., 2007. A comparison of four geophysical methods for determining the shear wave velocity of soils. Environmental and Engineering Geoscience, 13(1), 11–23. https://doi.org/10.2113/gseegeosci.13.1.11

ASTM D4428/D4428M-14, 2014. "Standard Test Methods for Crosshole Seismic Testing," ASTM International

ASTM D7400-14, 2018. "Standard Test Methods for Downhole Seismic Testing" ASTM International.

Baban, E. N., Amin, A. K. and Mohammed, S. S., 2022. Seismic Refraction Tomography and Geotechnical Parameters to Assess the Chaqchaq Dam failure in NW Sulaimani City, Kurdistan Region, Iraq. Iraqi National Journal of Earth Science, 22(2), 121-139. https://doi.org/10.33899/EARTH.2022.135251.1027 .

Dietrich, P. and Tronicke, J., 2009. Integrated analysis and interpretation of cross-hole P-and S-wave tomograms: A case study. Near Surface Geophysics, 7(2), 101–109. https://doi.org/10.3997/1873-0604.2008041

Dobry, R., Borcherdt, R. D., Crouse, C. B., Idriss, I. M., Joyner, W. B., Martin, G. R., Power, M. S., Rinne, E. E. and Seed, R. B., 2000. New Site Coefficients and Site Classification System Used in Recent Building Seismic Code Provisions. Earthquake Spectra, 16(1), 41–67. https://doi.org/10.1193/1.1586082

Fauzi, A., Irsyam, M. and Fauzi, U. J., 2014. Empirical correlation of shear wave velocity and N-SPT value for Jakarta. GEOMATE Journal, 7(13), 980–984. https://geomatejournal.com/geomate/article/view/2989

Foti, S., 2012. Combined use of Geophysical Methods for Geotechnical Site Characterization. 4th International Conference on Geotechnical and Geophysical Site Characterization, Recife, Brazil – September 2012.

Foti, S., Lai, C. G., Rix, G. J. and Strobbia, C., 2014. Surface Wave Methods for Near-Surface Site Characterization. CRC Press, London, p 487. https://doi.org/10.1201/b17268

Foti, S., Parolai, S., Albarello, D. and Picozzi, M., 2011. Application of Surface-Wave Methods for Seismic Site Characterization. Surveys in Geophysics, 32(6), 777–825. https://doi.org/10.1007/s10712-011-9134-2

Garofalo, F., Foti, S., Hollender, F., Bard, P. Y., Cornou, C., Cox, B. R., Dechamp, A., Ohrnberger, M., Perron, V., Sicilia, D., Teague, D. and Vergniault, C., 2016a. Inter PACIFIC project: Comparison of invasive and non-invasive methods for seismic site characterization. Part II: Inter-comparison between surface-wave and borehole methods. Soil Dynamics and Earthquake Engineering, 82, 241–254. https://doi.org/10.1016/j.soildyn.2015.12.009

Garofalo, F., Foti, S., Hollender, F., Bard, P. Y., Cornou, C., Cox, B. R., Ohrnberger, M., Sicilia, D., Asten, M., Di Giulio, G., Forbriger, T., Guillier, B., Hayashi, K., Martin, A., Matsushima, S., Mercerat, D., Poggi, V. and Yamanaka, H., 2016b. Inter PACIFIC project: Comparison of invasive and non-invasive methods for seismic site characterization. Part I: Intra-comparison of surface wave methods. Soil Dynamics and Earthquake Engineering, 82, 222–240. https://doi.org/10.1016/j.soildyn.2015.12.010

Honjo, Y., 2011. Challenges in geotechnical reliability-based design. Geotechnical Safety and Risk. ISGSR 2011 - Vogt, Schuppener, Straub and Bräu (eds), 11-27.

Hussien, M. N. and Karray, M., 2015. Shear wave velocity as a geotechnical parameter: An overview. Canadian Geotechnical Journal, 53(2), 252–272. https://doi.org/10.1139/cgj-2014-0524

Ivanov, J., Miller, R. D., Morton, S. and Peterie, S., 2015. Dispersion-Curve Imaging Considerations When Using Multichannel Analysis of Surface Wave (MASW) Method. Symposium on the Application of Geophysics to Engineering and Environmental Problems 2015, 556–566. https://doi.org/10.4133/SAGEEP.28-079.

Kearey, P., Brooks, M. and Hill, I., 2002. An introduction to geophysical exploration (Vol. 4). John Wiley and Sons. 288 p.

Kim, D.-S., Bang, E.-S. and Kim, W.-C., 2004. Evaluation of various downhole data reduction methods for obtaining reliable V s profiles. Geotechnical Testing Journal, 27(6), 585–597. https://doi.org/10.1520/GTJ11811

Kramer, S. L., 2014. Geotechnical Earthquake Engineering. Pearson; 1st ed., Pearson. 653 p.

Kumar, A., Panjamani, A., Kumar, R. and Lenin, K. R., 2023. Study of Shallow Soil Deposit in East Coast of India by SPT, MASW, and Crosshole Tests. In K. Muthukkumaran, R. Ayothiraman, and S. Kolathayar (Eds.), Soil Dynamics, Earthquake and Computational Geotechnical Engineering (Vol. 300, pp. 391–404). Springer Nature Singapore. https://doi.org/10.1007/978-981-19-6998-0_33.

L'Heureux, J.-S. and Long, M., 2017. Relationship between shear-wave velocity and geotechnical parameters for Norwegian clays. Journal of Geotechnical and Geoenvironmental Engineering, 143(6), 04017013. https://doi.org/10.1061/(ASCE)GT.1943-5606.0001645 .

Lebedev, M. and Dorokhin, K., 2019. Application of cross-hole tomography for assessment of soil stabilization by grout injection. Geosciences, 9(9), 399. https://doi.org/10.3390/geosciences9090399

Liu, H.-P., 2000. Comparison of Phase Velocities from Array Measurements of Rayleigh Waves Associated with Microtremor and Results Calculated from Borehole Shear-Wave Velocity Profiles. Bulletin of the Seismological Society of America, 90(3), 666–678. https://doi.org/10.1785/0119980186

Look, B. G., 2014. Handbook of geotechnical investigation and design tables. CRC Press. 418p.

Luo, Y., Xia, J., Liu, J., Xu, Y. and Liu, Q., 2009. Research on the middle-of-receiver-spread assumption of the MASW method. Soil Dynamics and Earthquake Engineering, 29(1), 71–79. https://doi.org/10.1016/j.soildyn.2008.01.009

Martínez-Pagán, P., Navarro, M., Pérez-Cuevas, J., Alcalá, F. J., García-Jerez, A. and Vidal, F. rancisco., 2018. Shear-wave velocity structure from MASW and SPAC methods: The case of Adra town, SE Spain. Near Surface Geophysics, 16(3), 356–371. https://doi.org/10.3997/1873-0604.2018012.

Miller, R. D., Xia, J., Park, C. B. and Ivanov, J. M., 1999. Multichannel analysis of surface waves to map bedrock. The Leading Edge, 18(12), 1337–1448. https://doi.org/10.1190/1.1438226

Mok, Y. J., Park, C. S. and Nam, B. H., 2016. A borehole seismic source and its application to measure in-situ seismic wave velocities of geo-materials. Soil Dynamics and Earthquake Engineering, 80, 127–137. https://doi.org/10.1016/j.soildyn.2015.10.011

Moon, S.-W. and Ku, T., 2016. Development of global correlation models between in situ stress-normalized shear wave velocity and soil unit weight for plastic soils. Canadian Geotechnical Journal, 53(10), 1600–1611. https://doi.org/10.1139/cgj-2016-0015

Olafsdottir, E. A., Erlingsson, S. and Bessason, B., 2018. Tool for analysis of multichannel analysis of surface waves (MASW) field data and evaluation of shear wave velocity profiles of soils. Canadian Geotechnical Journal, 55(2), 217-233. https://doi.org/10.1139/cgj-2016-0302

Park, C. B., Miller, R. D. and Xia, J., 1998. Imaging dispersion curves of surface waves on multi-channel record. SEG Technical Program Expanded Abstracts 1998, 1377–1380. https://doi.org/10.1190/1.1820161

Park, C. B., Miller, R. D. and Xia, J., 1999. Multichannel analysis of surface waves. GEOPHYSICS, 64(3), 800–808. https://doi.org/10.1190/1.1444590

Phoon, K.-K. and Kulhawy, F. H., 1999. Evaluation of geotechnical property variability. Canadian Geotechnical Journal, 36(4), 625–639. https://doi.org/10.1139/t99-039 .

Poulos, H. G., 2018. A review of geological and geotechnical features of some Middle Eastern countries. Innovative Infrastructure Solutions, 3(1), 51. https://doi.org/10.1007/s41062-018-0158-z

Price, S. J., Farrant, A. R., Thomas, R. J. and Ellison, R. A., 2012. Geology of the Dubai, Sharjah and Sir Bu N'Air 1:100 000 map sheet, 100-5, United Arab Emirates. British Geological Survey.

Sairam, B., Singh, A. P., Patel, V., Chopra, S. and Kumar, M. R., 2019. Vs 30 mapping and site characterization in the seismically active intraplate region of Western India: Implications for risk mitigation. Near Surface Geophysics, 17(5), 533–546. https://doi.org/10.1002/nsg.12066

Socco, L. V. and Strobbia, C., 2004. Surface-wave method for near-surface characterization: A tutorial. Near Surface Geophysics, 2(4), 165–185. https://doi.org/10.3997/1873-0604.2004015

Socco, L. V., Foti, S. and Boiero, D., 2010. Surface-wave analysis for building near-surface models—Established approaches and new perspectives. GEOPHYSICS, 75(5), 75A83-75A102. https://doi.org/10.1190/1.3479491

Stephenson, W. J., 2005. Blind Shear-Wave Velocity Comparison of ReMi and MASW Results with Boreholes to 200 m in Santa Clara Valley: Implications for Earthquake Ground-Motion Assessment. Bulletin of the Seismological Society of America, 95(6), 2506–2516. https://doi.org/10.1785/0120040240

Taylor, R. W., 1999. A Practical Guide to Borehole Geophysics in Environmental Investigations. Ground Water, 37(2), P.170

Wair, B. R., DeJong, J. T. and Shantz, T., 2012. Guidelines for Estimation of Shear Wave Velocity Profiles. Pacific Earthquake Engineering Research Center.

Xia, J., Miller, R. D. and Park, C. B., 1999. Estimation of near-surface shear-wave velocity by inversion of Rayleigh waves. GEOPHYSICS, 64(3), 691–700. https://doi.org/10.1190/1.1444578

Xia, J., Miller, R. D., Park, C. B., Hunter, J. A. and Harris, J. B., 2000. Comparing Shear-Wave Velocity Profiles from MASW with Borehole Measurements in Unconsolidated Sediments, Fraser River Delta, B.C., Canada. Journal of Environmental and Engineering Geophysics, 5(3), 1–13. https://doi.org/10.4133/JEEG5.3.1

Xia, J., Miller, R. D., Park, C. B., Hunter, J. A., Harris, J. B. and Ivanov, J., 2002a. Comparing shear-wave velocity profiles inverted from multichannel surface wave with borehole measurements. Soil Dynamics and Earthquake Engineering, 22(3), 181–190. https://doi.org/10.1016/S0267-7261(02)00008-8

Xia, J., Miller, R. D., Park, C. B., Hunter, J. A., Harris, J. B. and Ivanov, J., 2002b. Comparing shear-wave velocity profiles inverted from multichannel surface wave with borehole measurements. Soil Dynamics and Earthquake Engineering, 22(3), 181–190. https://doi.org/10.1016/S0267-7261(02)00008-8

Xia, J., Xu, Y. and Miller, R. D., 2007. Generating an Image of Dispersive Energy by Frequency Decomposition and Slant Stacking. Pure and Applied Geophysics, 164(5), 941–956. https://doi.org/10.1007/s00024-007-0204-9

Xie, J., Huang, J., Lu, J., Burton, G. J., Zeng, C. and Wang, Y., 2022. Development of two-dimensional ground models by combining geotechnical and geophysical data. Engineering Geology, 300, 106579. https://doi.org/10.1016/j.enggeo.2022.106579.